

## Structural Chemistry and Magnetic Behavior of Ternary Gallides $REAu_xGa_{4-x}$ , $RE = La, Ce, Pr, Nd, \text{ and } Sm^*$

Y. N. GRIN, P. ROGL, AND K. HIEBL

*Institut für Physikalische Chemie der Universität Wien, Währingerstrasse  
42, A-1090 Vienna, Austria*

F. E. WAGNER

*Physik Department EI, Technische Universität München,  
James Franck-Strasse, D-8046 Garching, Federal Republic of Germany*

AND H. NOËL

*Laboratoire de Chimie du Solide B, Université de Rennes I,  
Avenue du General Leclerc, F-35042, Rennes, France*

Received December 20, 1986

Two new series of ternary gallides with the chemical formulas  $(La, Ce, Pr, Nd, Sm)Au_xGa_{4-x}$  and  $(La, Ce, Pr, Nd, Sm)Au_{1.5}Ga_{2.5}$  were synthesized from the elements by arc melting. From X-ray powder diffraction analysis the  $REAu_xGa_{4-x}$  series of compounds was found to be isotypic and crystallize with  $BaAl_4$  type of structure; the homogeneity range at 600°C of each of the  $REAu_xGa_{4-x}$  phases was established, revealing remarkable deviations from Vegard's rule. At 600°C the  $REAu_xGa_{4-x}$  phases of the  $BaAl_4$  type were observed to be in thermodynamic equilibrium with a structure variant crystallizing at the composition  $REAu_{1.5}Ga_{2.5}$  and with a narrow homogeneous range. In case of  $PrAu_{1.5}Ga_{2.5}$  the structure type was refined from X-ray single-crystal counter data ( $CaBe_2Ge_2$  type, space group  $P4/nmm$ ,  $R_w = 0.046$ ). Gold and gallium atoms were generally found on separate crystallographic sites; however, a statistical distribution of 51% Au + 49% Ga was derived for the  $2b$  sites.  $^{197}Au$  Mössbauer spectroscopy confirmed the occupational mode of the gold atoms in  $CeAu_{1.5}Ga_{2.5}$ . For the  $BaAl_4$ -type phases, X-ray powder and Mössbauer data revealed preferential occupation of the  $4e$  sites of  $I4/mmm$  by gold atoms; practically no Au was observed on the  $4d$  sites. Magnetic susceptibilities were determined over a temperature range extending from 2 to 1100 K. Above liquid nitrogen temperatures the paramagnetic behavior of the  $(Ce, Pr, Nd)Au_xGa_{4-x}$  and the  $(Ce, Pr, Nd)Au_{1.5}Ga_{2.5}$  compounds is characterized by magnetic moments close to the ideal trivalent rare earth values. Lanthanum compounds are diamagnetic, whereas  $SmAu_xGa_{4-x}$  alloys are characterized by a typical Van Vleck-type paramagnetism of closely spaced multiplets. At very low temperatures onset of ferromagnetic ordering is observed for the  $BaAl_4$ -type series of compounds. No superconductivity was encountered down to 2 K. © 1987 Academic Press, Inc.

\* Dedicated to Dr. H. Nowotny.

## 1. Introduction

In continuation of our general program (1–3) concerning the stabilization of  $BaAl_4$  and derivative types of structure among ternary rare earth gallides  $REM_xGa_{4-x}$ , where  $M$  represents one of the platinum or noble metals, respectively, we have now concentrated our interest on the alloy systems  $REAu_xGa_{4-x}$ , where  $RE$  is one of the light (ceric) rare earth metals.

## 2. Experimental

All samples, each of a total amount of ca. 1 g and with variable ratios of Au to Ga were synthesized by arc melting the high-purity elements together in a Ti/Zr-gettered argon atmosphere starting from nominal atomic compositions  $RE:(Au,Ga) = 1:4$ . Weight losses due to the arc melting process were verified to be less than 1 wt%. The impurity level of the starting materials, further details of sample preparation and heat treatments employed (170 hr at 600°C in evacuated silica tubes), X-ray techniques applied, and a general description of the magnetic measurements (80 K <  $T$  < 1100 K) can be found in preceding publications on a similar subject (1, 2). The low-temperature magnetization (2 K <  $T$  < 300 K) was measured on a SQUID magnetometer employing a superconducting solenoid for fields up to 5 T. No superconductivity was observed down to 2 K.

A small single-crystal specimen suitable for X-ray diffraction was obtained by mechanical fragmentation of an arc-melted alloy with the nominal composition Pr(20 at.%)Au(30)Ga(50), after annealing for 170 hr at 600°C. Lattice parameters and intensities were measured with graphite monochromatized  $MoK\alpha$  radiation on a STOE (Siemens) automatic four-circle diffractometer. The cell parameters were determined from a least-squares refinement of high angle  $2\theta$  values of 22 reflections. The

crystallographic data are listed in Table I. A total of 1064 reflections were recorded up to a limit of  $\sin \theta/\lambda = 0.81 \text{ \AA}^{-1}$ . A set of 302 symmetry-independent intensities was obtained by averaging "centered reflections" only, and all observed intensities (214 for which  $|F_o| > 3\sigma$ ) were used in the structure refinement. An empirical absorption correction was applied using  $\Psi$  scans of two independent reflections.

Mössbauer spectra were recorded at 4.2 K with a standard constant acceleration-type spectrometer and a source of  $^{197}\text{Pt}$  in enriched  $^{196}\text{Pt}$  metal. The spectra were least-squares fitted with suitable superpositions of Lorentzian line shapes.

## 3. Results and Discussion

### 3.1. The Crystal Structure of $SmAu_{1.15}Ga_{2.85}$ ( $BaAl_4$ -Type) and Isotypic Compounds $REAu_xGa_{4-x}$

Single-crystal fragments obtained by mechanical fragmentation of an arc-melted alloy Sm(20 at.%)Au(23)Ga(57) annealed for 170 hr at 600°C were extremely small for X-ray diffraction analysis. X-ray Laue and rotation photographs along the two crystal axes [001] and [100], however, confirmed the tetragonal high Laue symmetry  $4/mmm$ ; heavily exposed rotation photographs further did not reveal any significant indications for superstructure formation. Indexation of the rotation and Guinier powder photographs was complete on the basis of a body centered-tetragonal unit cell, suggesting isotypism with the structure type of  $BaAl_4$ . Powder intensity calculations unambiguously revealed that the gold atoms, i.e., the heavy X-ray scatterers, were preferentially located in the  $4e$  sites in form of a statistical Au/Ga occupation.

X-ray powder patterns of alloys  $REAu_xGa_{4-x}$  in the concentration range  $0.3 < x < 1.3$  confirmed the existence of new compounds with  $RE = \text{La, Ce, Pr, Nd, and Sm}$ .

TABLE I  
CRYSTALLOGRAPHIC AND MAGNETIC DATA OF  $REAu_xGa_{4-x}$  COMPOUNDS

Composition (at.%)	Cell dimensions (Å)				$\theta_p$ K	$\mu_{\text{eff}}$ (BM)		Ferromagn. Curie temp. $T_M$ , K
	<i>a</i>	<i>c</i>	<i>V</i>	<i>c/a</i>		Obs.	Theor. $RE^{3+}$	
$La_{20}Au_4Ga_{76}^a$	4.406(1)	10.231(3)	198.6(1)	2.322				
$La_{20}Au_7Ga_{73}$	4.405(1)	10.384(4)	201.5(1)	2.357				
$La_{20}Au_9Ga_{71}$	4.403(1)	10.531(4)	204.1(1)	2.392				
$La_{20}Au_{12}Ga_{68}$	4.396(1)	10.568(5)	204.2(1)	2.404				
$La_{20}Au_{13.5}Ga_{64.5}$	4.392(1)	10.579(3)	204.1(1)	2.409				
$La_{20}Au_{17}Ga_{63}$	4.379(1)	10.633(3)	203.9(1)	2.428				
$La_{20}Au_{23}Ga_{57}^a$	4.379(1)	10.632(2)	203.9(1)	2.428				
$La_{20}Au_{30}Ga_{50}^b$	4.379(1)	10.632(2)	203.9(1)	2.428				
$Ce_{20}Au_4Ga_{76}^a$	4.364(1)	10.134(3)	193.0(1)	2.322				
$Ce_{20}Au_7Ga_{73}$	4.364(1)	10.282(4)	195.8(1)	2.356	17	2.44	2.54	
$Ce_{20}Au_{10}Ga_{70}$	4.361(2)	10.459(5)	198.9(2)	2.398	16	2.45	2.54	
$Ce_{20}Au_{12}Ga_{68}$	4.353(2)	10.586(9)	200.6(2)	2.432	15	2.47	2.54	6
$Ce_{20}Au_{15}Ga_{65}$	4.343(1)	10.641(3)	200.7(1)	2.450	6	2.55	2.54	4.5
$Ce_{20}Au_{20}Ga_{60}$	4.340(2)	10.663(4)	200.8(2)	2.457	8	2.59	2.54	3.5
$Ce_{20}Au_{22}Ga_{58}$	4.335(2)	10.699(3)	201.0(2)	2.468				
$Ce_{20}Au_{27}Ga_{53}^a$	4.330(2)	10.726(6)	201.1(2)	2.477				
$Ce_{20}Au_{30}Ga_{50}^b$	4.349(2)	10.671(6)	201.9(2)	2.454	-1	2.64	2.54	c
$Pr_{20}Au_6Ga_{74}^a$	4.334(1)	10.096(3)	189.7(1)	2.329				
$Pr_{20}Au_{10}Ga_{70}$	4.337(1)	10.376(8)	195.2(2)	2.392				
$Pr_{20}Au_{12}Ga_{68}$	4.325(1)	10.516(4)	196.7(1)	2.432				
$Pr_{20}Au_{15}Ga_{65}$	4.320(1)	10.653(3)	198.9(1)	2.466	27	3.44	3.58	7
$Pr_{20}Au_{19}Ga_{61}$	4.314(1)	10.680(4)	198.8(1)	2.475				
$Pr_{20}Au_{24}Ga_{56}$	4.313(1)	10.699(2)	199.1(1)	2.481				
$Pr_{20}Au_{27}Ga_{53}^a$	4.309(1)	10.739(4)	199.4(1)	2.492				
$Pr_{20}Au_{30}Ga_{50}^b$	4.324(1)	10.682(4)	199.6(1)	2.471	14	3.58	3.58	c
$Nd_{20}Au_7Ga_{73}^a$	4.324(1)	10.031(5)	187.5(1)	2.320				
$Nd_{20}Au_{12}Ga_{68}$	4.312(1)	10.301(5)	191.5(1)	2.389				
$Nd_{20}Au_{15}Ga_{65}$	4.300(1)	10.529(6)	194.7(2)	2.449				
$Nd_{20}Au_{17}Ga_{63}$	4.290(2)	10.700(8)	196.9(2)	2.404				
$Nd_{20}Au_{20}Ga_{60}$	4.289(1)	10.726(3)	197.3(1)	2.501	9	3.49	3.62	4
$Nd_{20}Au_{24}Ga_{56}$	4.290(1)	10.732(3)	197.4(1)	2.501				
$Nd_{20}Au_{27}Ga_{53}^a$	4.287(1)	10.748(3)	197.5(1)	2.507				
$Nd_{20}Au_{30}Ga_{50}^b$	4.303(1)	10.705(3)	198.2(1)	2.488	10	3.49	3.62	c
$Sm_{20}Au_7Ga_{73}^a$	4.280(1)	10.009(2)	183.3(1)	2.339				
$Sm_{20}Au_{11}Ga_{69}$	4.283(1)	10.173(2)	186.6(2)	2.376				
$Sm_{20}Au_{15}Ga_{65}$	4.259(1)	10.598(4)	192.2(1)	2.488				
$Sm_{20}Au_{19}Ga_{61}$	4.251(1)	10.809(1)	195.3(1)	2.543	—	1.57 <sup>d</sup>	1.60 <sup>d</sup>	
$Sm_{20}Au_{23}Ga_{57}$	4.238(1)	10.845(3)	194.8(1)	2.559				
$Sm_{20}Au_{27}Ga_{53}^a$	4.247(1)	10.818(3)	195.1(1)	2.547				
$Sm_{20}Au_{32}Ga_{48}^b$	4.255(1)	10.791(5)	195.4(1)	2.536				

<sup>a</sup> Samples were multiphase.

<sup>b</sup> Samples had  $CaBe_2Ge_2$  structure.

<sup>c</sup> No magnetic ordering observed down to 2 K.

<sup>d</sup> Values at 300 K.

$$\chi_M(300\text{ K}) = -2.42 \times 10^{-4} \text{ cm mole}^{-1}$$

From the practically analogous X-ray photographs, structural identity with  $SmAu_{1.15}Ga_{2.85}$  is concluded (see above). The precise distribution of the gold atoms on the available crystallographic sites  $4d$ ,  $4e$  was monitored by  $^{197}Au$  Mössbauer spectroscopy for the  $CeAu_xGa_{4-x}$  alloys and for various compositions (see Section 3.3).

For each of the above-mentioned rare earth members the homogeneous range of existence at  $600^\circ C$  was determined from X-ray phase analysis (see Fig. 1 and Table I). Except for the La–Au–Ga system the homogeneous ranges are practically constant; their range of existence, however, is much wider than for the homologous  $REAg_xGa_{4-x}$  compounds (3). The monotonous nonlinear variation of the unit cell dimensions versus composition (Fig. 1) is correlated to the complex substitution mode of the Au, Ga atoms in the structure (see Section 3.3).

No formation of  $REAu_xGa_{4-x}$  compounds was observed in our experiments with the

heavier rare earth members, i.e.,  $RE = Gd, Tb, \text{ or } Dy$ .

### 3.2. The Crystal Structure of $PrAu_{1.5}Ga_{2.5}$ ( $CaBe_2Ge_2$ -Type) and Isotypic Compounds $REAu_{1.5}Ga_{2.5}$ ( $RE = La, Ce, Nd, \text{ and } Sm$ )

X-ray Guinier powder photographs of  $REAu_xGa_{4-x}$  alloys with higher Au contents prove the existence of new compounds for  $RE = La, Ce, Pr, Nd, \text{ and } Sm$  with a rather narrow range of homogeneity around  $x \approx 1.5$ . All observed diffractograms are completely indexed on the basis of a primitive tetragonal unit cell, and crystallographic data are listed in Table I. Composition, lattice parameters, and the observed extinctions ( $hk0$ ) for  $h + k = 2n + 1$  are compatible with the  $CaBe_2Ge_2$  type of structure and a statistical test clearly confirmed the existence of a center of symmetry. Further refinement was therefore performed in space group  $P4/nmm$  with the highest symmetry, employing the STRUCSY full-matrix least-squares program system (STOE and CIE, Darmstadt). The weights used were  $w_i = 1/\{\sigma(F_i)^2\}$ ; different weighting schemes had no significant influence on the  $R$  values obtained. The least-squares refinement in combination with a Fourier difference calculation  $|F_o - F_c|$  unambiguously revealed the atom order as derived in Table II.

Refinement of the occupancy parameters confirmed the partially ordered atom distribution and within the errors of the calculation proved a full occupation for the Pr, Au(1), Ga(2), and Ga(3) sites, whereas a statistical distribution of 1.02 Au(2) and 0.98 Ga(1) was obvious on the  $2b$  sites in  $3/4, 1/4, 1/2$ . The final atom parameters calculated with isotropic extinction and anisotropic thermal parameters to a reliability factor  $R = 0.057$  ( $R_w = 0.046$ ) are given in Table II; a comparison of  $|F_o|$  and  $|F_c|$  data is presented in Table III and interatomic distances up to  $4.0 \text{ \AA}$  are given in Table IV.

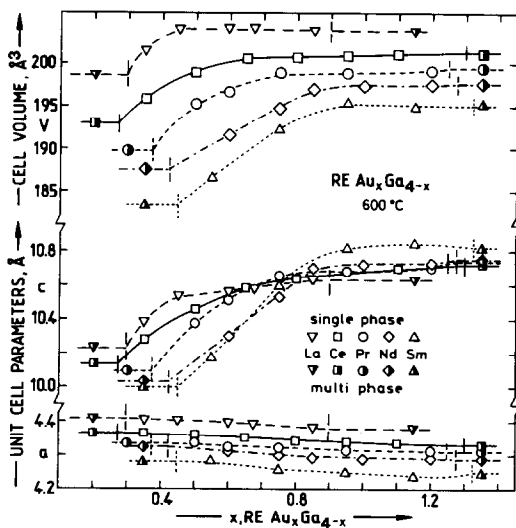


FIG. 1. Unit cell dimensions of alloys  $REAu_xGa_{4-x}$  ( $BaAl_4$  type;  $RE = La, Ce, Pr, Nd, Sm$ ) versus concentration  $0.2 < x < 1.4$ ; the homogeneous ranges at  $600^\circ C$  are indicated by vertical bars.

TABLE II  
CRYSTALLOGRAPHIC DATA FOR Pr(Au<sub>0.75</sub>Ga<sub>0.25</sub>)<sub>2</sub>Ga<sub>2</sub> (CaBe<sub>2</sub>Ge<sub>2</sub> TYPE)

Atom	Site	x	y	z	U <sub>eq.</sub>	U <sub>11</sub>	U <sub>22</sub>	U <sub>33</sub>
Pr	2c	3/4	3/4	0.7491(2)	0.93	0.64(7)	0.64(7)	1.51(7)
Au(1)	2c	3/4	3/4	0.1311(2)	1.44	1.13(7)	1.13(7)	2.07(8)
1.02(2)Au(2) + 0.98(2)Ga(1)	2b	3/4	1/4	1/2	1.48	1.46(12)	1.46(12)	1.51(10)
Ga(2)	2c	3/4	3/4	0.3673(5)	0.90	0.55(18)	0.55(18)	1.60(17)
Ga(3)	2a	3/4	1/4	0	1.12	0.88(20)	0.88(20)	1.58(18)

Note. Space group  $P4/nmm$ ,  $D_{4h}^7$ , No. 129, origin at center; standard deviations are in parentheses;  $a = 4.3235(8)$  Å,  $c = 10.6823(44)$  Å,  $cla = 2.471$ ,  $V = 199.68$  Å<sup>3</sup>;  $D_x = 10.13$  Mg m<sup>-3</sup>,  $\mu(\text{MoK}\alpha) = 80.1$  mm<sup>-1</sup>,  $R = 0.057$ ,  $R_w = 0.046$ . Anisotropic thermal factors are of the form:  $T = \exp[-2\pi^2(U_{11}h^2a^{*2} + U_{22}k^2b^{*2} + U_{33}l^2c^{*2} + 2U_{12}hka^*b^* + \dots) \times 10^{-2}]$ ; by symmetry  $U_{12} = U_{13} = U_{23} = 0$ . Correction for secondary extinction was  $1.5(4) \times 10^{-6}$ .

TABLE III  
OBSERVED AND CALCULATED STRUCTURE FACTORS FOR Pr(Au<sub>0.75</sub>Ga<sub>0.25</sub>)<sub>2</sub>Ga<sub>2</sub>

h	k	l	10F <sub>0</sub>	10F <sub>c</sub>	h	k	l	10F <sub>0</sub>	10F <sub>c</sub>	h	k	l	10F <sub>0</sub>	10F <sub>c</sub>	h	k	l	10F <sub>0</sub>	10F <sub>c</sub>	h	k	l	10F <sub>0</sub>	10F <sub>c</sub>
1	1	0	1482	-1380	0	2	0	3422	-3662	2	2	0	3372	3044	1	3	0	1069	1015	3	3	0	868	-841
0	4	0	2281	2367	2	4	0	2290	-2110	1	5	0	706	-723	3	5	0	617	633	0	6	0	1356	-1466
2	6	0	1388	1349	0	0	1	99	152	0	1	1	417	410	1	1	1	863	-943	0	2	1	160	-132
1	2	1	335	-332	0	3	1	311	-280	1	3	1	623	652	2	3	1	305	236	3	3	1	497	-504
1	4	1	234	200	0	5	1	187	149	1	5	1	424	-405	3	5	1	327	331	0	0	2	367	360
0	1	2	706	830	1	1	2	2392	2419	0	2	2	254	-263	1	2	2	623	-676	2	2	2	212	202
0	3	2	505	-580	1	3	2	1775	-1706	2	3	2	475	511	3	3	2	1413	1334	0	4	2	179	110
1	4	2	448	457	3	4	2	388	-375	0	5	2	363	375	1	5	2	1057	1086	2	5	2	318	-342
3	5	2	883	-906	4	5	2	297	262	1	6	2	275	-286	0	0	3	939	-1044	0	1	3	2018	2009
0	2	3	763	837	1	2	3	1740	-1658	2	2	3	705	-709	0	3	3	1433	-1439	2	3	3	1374	1273
0	4	3	508	-546	1	4	3	1206	1147	2	4	3	528	488	3	4	3	975	-975	4	4	3	368	-358
0	5	3	895	953	2	5	3	900	-875	3	5	3	147	-101	4	5	3	647	697	0	6	3	326	324
1	6	3	706	-749	2	6	3	269	-293	3	6	3	608	650	0	0	4	614	584	1	1	4	1976	1929
0	2	4	482	-467	2	2	4	348	392	1	3	4	1447	-1386	2	3	4	199	-72	3	3	4	1138	1059
0	4	4	289	300	2	4	4	265	-267	1	5	4	803	840	3	5	4	673	-680	0	6	4	231	-180
2	6	4	185	166	0	0	5	745	-800	0	1	5	2077	-2044	0	2	5	635	667	1	2	5	1827	1744
2	2	5	599	-575	0	3	5	1503	1537	2	3	5	1469	-1372	3	3	5	238	60	0	4	5	441	-450
1	4	5	1248	-1242	2	4	5	390	403	3	4	5	1079	1038	4	4	5	291	-297	0	5	5	985	-1039
2	5	5	971	956	4	5	5	723	-764	0	6	5	227	269	1	6	5	780	821	2	6	5	239	-243
0	0	6	760	737	0	1	6	532	-572	1	1	6	1482	1422	0	2	6	597	-609	1	2	6	457	496
2	2	6	528	509	0	3	6	414	439	1	3	6	1141	-1080	2	3	6	381	-393	3	3	6	964	865
0	4	6	354	365	1	4	6	345	-356	2	4	6	325	-313	3	4	6	311	295	4	4	6	251	203
0	5	6	300	-295	1	5	6	719	715	2	5	6	291	269	3	5	6	595	-601	0	0	7	162	195
1	1	7	688	-760	0	2	7	141	-179	2	2	7	182	166	1	3	7	572	589	3	3	7	528	-474
0	5	7	177	83	1	5	7	385	-389	2	5	7	215	-81	3	5	7	330	320	0	0	8	2646	2572
1	1	8	772	-741	0	2	8	2250	-2255	2	2	8	2075	2004	1	3	8	649	631	3	3	8	618	-551
0	4	8	1598	1638	2	4	8	1576	-1490	4	4	8	1193	1160	1	5	8	488	-488	3	5	8	458	435
0	6	8	1013	-1075	1	6	8	189	-40	0	1	9	379	365	1	1	9	431	-425	1	2	9	330	-317
0	3	9	247	-278	1	3	9	337	335	2	3	9	259	245	3	3	9	312	-269	1	4	9	165	218
3	4	9	260	-175	1	5	9	241	-218	3	5	9	229	177	0	0	10	307	-123	0	1	10	400	403
1	1	10	1494	1494	0	2	10	130	131	1	2	10	364	-363	2	2	10	172	-173	0	3	10	338	-330
1	3	10	1205	-1212	2	3	10	355	301	3	3	10	1045	1007	1	4	10	307	275	3	4	10	299	-231
0	5	10	305	231	1	5	10	825	854	2	5	10	265	-212	0	0	11	519	-520	0	1	11	694	690
0	2	11	466	465	1	2	11	629	-631	2	2	11	435	-419	0	3	11	566	-580	2	3	11	549	535
0	4	11	370	-342	1	4	11	495	496	2	4	11	346	309	3	4	11	510	-430	0	5	11	414	431
0	0	12	370	372	0	1	12	140	-142	1	1	12	737	740	0	2	12	290	-335	1	2	12	128	130
2	2	12	270	303	1	3	12	592	-592	3	3	12	478	481	0	4	12	239	252	2	4	12	281	-231
3	4	12	171	84	0	0	13	311	-305	0	1	13	905	-910	0	2	13	270	275	1	2	13	809	837
2	2	13	274	-248	0	3	13	740	773	2	3	13	722	-716	0	4	13	251	-203	1	4	13	668	-665
0	0	14	425	415	0	1	14	233	-189	1	1	14	433	456	0	2	14	349	-370	1	2	14	227	173
2	2	14	332	331	0	3	14	153	158	1	3	14	392	-382	2	3	14	216	-144	0	4	14	205	266
0	1	15	169	199	1	1	15	359	-349	0	3	15	163	-177	1	3	15	308	288	0	0	16	871	876
1	1	16	198	-201	0	2	16	805	-809	1	2	16	134	-59										

TABLE IV  
INTERATOMIC DISTANCES IN  $PrAu_{1.5}Ga_{2.5}$  ( $<4.0$  Å)

Pr-4 Au	3.314(1)	Ga 1-4 Pr	3.429(2)
4 Ga 1 <sup>a</sup>	3.429(2)	4 Ga 1	3.057(4)
4 Ga 2	3.300(2)	4 Ga 2	2.585(3)
4 Ga 3	3.443(2)		
		Ga 2-4 Pr	3.300(2)
Au-4 Pr	3.314(1)	4 Ga 1	2.585(3)
1 Ga 2	2.523(5)	1 Au	2.523(5)
4 Ga 3	2.576(1)		
		Ga 3-4 Pr	3.443(2)
		4 Au	2.576(1)
		4 Ga 3	3.057(4)

<sup>a</sup> Ga 1 represents a statistical distribution of 1.02 Au + 0.98 Ga in the 2*b* sites (3/4, 1/4, 1/2); see Table II and Section 3.3.

$REAu_{1.5}Ga_{2.5}$  alloys, heat treated at 600°C, revealed the existence of a new phase with a narrow range of existence; calculated and observed X-ray powder intensities in all cases  $RE = La, Ce, Pr, Nd,$  and  $Sm$  were consistent with a  $CaBe_2Ge_2$ -type symmetry and confirmed the structural analogy with the atom order as derived from the single-crystal data of  $PrAu_{1.5}Ga_{2.5}$  (see Tables I, II).

### 3.3. $^{197}Au$ Mössbauer Spectroscopy

The 4.2 K Mössbauer spectra of the  $CeAu_xGa_{4-x}$  alloys were found virtually to represent a single absorption line for values  $x \leq 1.0$ , whereas for  $x = 1.5$  a shoulder is observed at smaller velocities (Fig. 2). The shape of the main peaks is Lorentzian. Perfect fits of the spectra could, however, be obtained by fitting symmetric quadrupole doublets; the quadrupole interaction obtained in this way is only about a quarter of the line width (Table V), but since its value hardly depends on  $x$  or absorber thickness, we consider deviations from the Lorentzian shape as attributable to hyperfine interactions rather than to saturation effects resulting from the finite absorber thickness.

The shoulder in the Mössbauer spectrum of  $CeAu_{1.5}Ga_{1.5}$  ( $CaBe_2Ge_2$  type) also requires a quadrupole doublet to be reproduced satisfactorily. A minimum error figure was achieved for an intensity ratio of  $Au(2c) : Au(2b) = 2.13(10)$ . Thus the Mössbauer data are in excellent accord with the occupational mode derived from X-ray data with 2 Au(1) in 2*c* and 1.04 Au(2) in the 2*b* sites of  $P4/nmm$  (ratio  $Au(2c) : Au(2b) = 1.96(4)$ ). Notably this argument neglects differences in the Lamb-Mössbauer factors for the two sites, but these are presumably minor.

For the phases with the  $BaAl_4$  structure ( $x = 0.6, 0.75$  and  $x = 1.00$ ) a single absorption line is observed, which shifts slightly to larger velocities with increasing  $x$ . It is not clear, however, whether the line broadening, which was interpreted as an unresolved quadrupole splitting, is really due to an electric quadrupole interaction or whether it arises from a distribution of isomer shifts. The latter could be caused by the statistical distribution of Au and Ga atoms in the neighborhood of the Au atoms. From the fact that all compounds with the  $BaAl_4$  ( $I4/mmm$ )-type structure exhibit a single peak, one may conclude that only a single crystallographic site (either 4*e* or 4*d*) is occupied by the gold atoms. Since theoretical estimates of the isomer shifts of gold on these sites cannot be made, Mössbauer spectroscopy cannot determine which of these sites is occupied. We estimate that, if Au on the two sites is indeed distinguishable in the Mössbauer spectrum by the hyperfine interactions, about 2% occupancy of the minority site could have been detected.

Model calculations of the X-ray powder diagrams, however, clearly indicate a preferential occupation of the 4*e* sites by the gold atoms (see Section 3.1). The main peak of the Mössbauer spectrum is thus unambiguously due to Au in the 4*e* sites of  $I4/mmm$ . Furthermore only a minor occu-

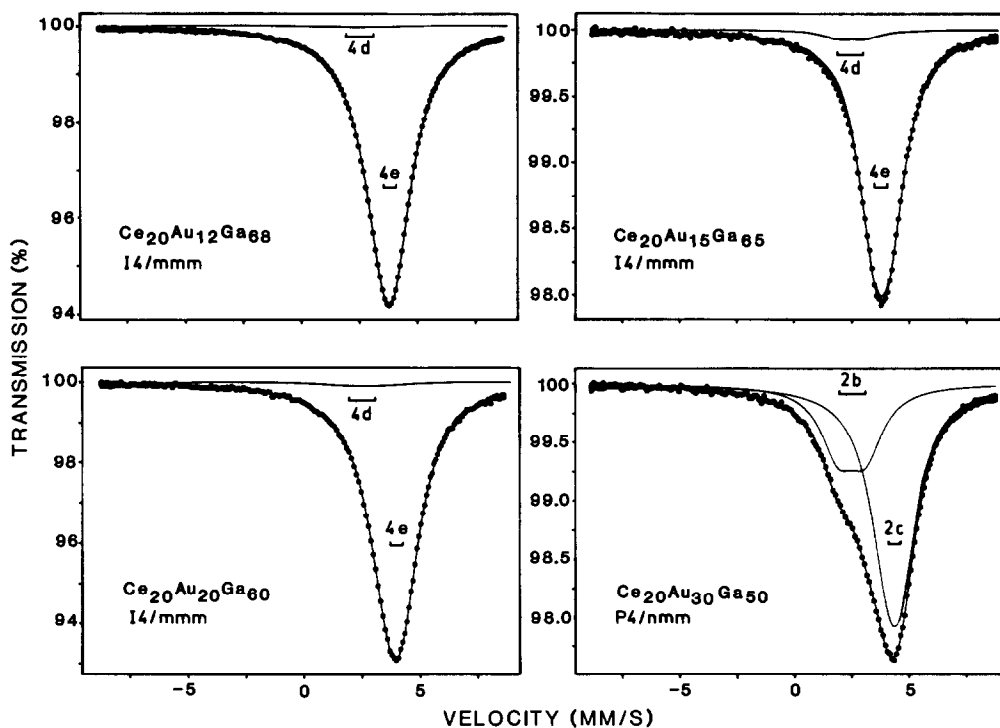


FIG. 2. Room temperature Mössbauer spectra of  $\text{CeAu}_x\text{Ga}_{4-x}$  alloys; solid circles, experimental data; solid line, calculated profile; solid bars, the Au contributions from the different Au sublattice sites.

pation of the  $4d$  sites by Au atoms is revealed by Mössbauer spectroscopy, in good correspondence to the homologous alloy system  $\text{CeAg}_x\text{Ga}_{4-x}$  (2) and was also

observed for  $\text{CePd}_x\text{Ga}_{4-x}$  (3). The retrograde character of the Au occupation in the  $4d$  sites together with a successive filling of the  $4e$  sites by gold atoms is therefore

TABLE V  
MÖSSBAUER DATA FOR  $\text{CeAu}_x\text{Ga}_{4-x}$  ALLOYS

Alloy	$\Gamma$ (mg Au/cm <sup>2</sup> )	$W$ (mm/sec)	IS (mm/sec)	$\Delta E_Q$ (mm/sec)	$I$	Structure type/ space group	Atom site
$\text{CeAu}_{0.60}\text{Ga}_{3.40}$	53.6	2.02(1)	3.76(2)	0.52(2)	0.99	$\text{BaAl}_4$	1.20 Au + 2.80 Ga in $4e$
			2.53 <sup>a</sup>	1.20 <sup>a</sup>	0.01(1)	$I4/mmm$	0.01(3) Au + 3.99 Ga in $4d$
$\text{CeAu}_{0.75}\text{Ga}_{3.25}$	34.1	1.81(2)	3.80(2)	0.60(2)	0.96	$\text{BaAl}_4$	1.43 Au + 2.57 Ga in $4e$
			2.53 <sup>a</sup>	1.20 <sup>a</sup>	0.04(1)	$I4/mmm$	0.06(3) Au + 3.94 Ga in $4d$
$\text{CeAu}_{1.00}\text{Ga}_{3.00}$	54.7	2.10(2)	3.93(2)	0.59(2)	0.98	$\text{BaAl}_4$	1.96 Au + 2.04 Ga in $4e$
			2.53 <sup>a</sup>	1.20 <sup>a</sup>	0.02(1)	$I4/mmm$	0.04(3) Au + 3.96 Ga in $4d$
$\text{CeAu}_{1.50}\text{Ga}_{2.50}$	34.4	1.84(2)	4.36(2)	0.58(3)	0.68	$\text{CaBe}_2\text{Ge}_2$	2 Au in $2c$
			2.53(4)	1.20(4)	0.32(1)	$P4/nmm$	0.94(5) Au + 1.06 Ga in $2b$

Note. Hyperfine parameters as derived from the computer fit described in text;  $W$  is the line width;  $\Gamma$  represents the FWHM-absorber cross section,  $I$  equals the relative intensity of the peaks, IS is the isomer shift relative to the Pt metal source, and  $\Delta E_Q$  is the quadrupole splitting (full-doublet separation).

<sup>a</sup> Value restricted in refinement.

<sup>b</sup> A least-squares refinement of the  $\text{CuK}\alpha$  X-ray powder diffraction pattern of  $\text{CeAuGa}_3$  revealed 2.04(10)Au + 1.96(10)Ga in  $4e$  and 0.08(12)Au + 3.92(12)Ga in  $4d$ ,  $I4/mmm$ ,  $R_I = 0.075$ .

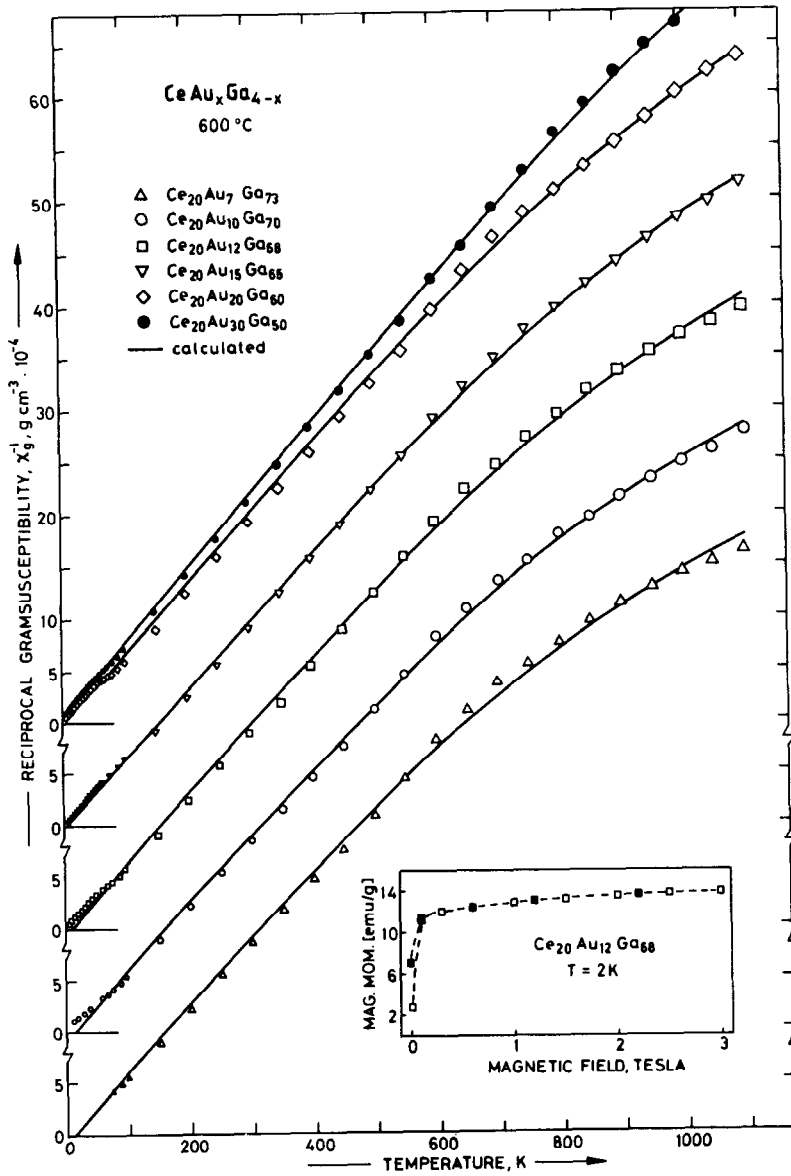


FIG. 3. Reciprocal gram-susceptibility versus temperature for  $CeAu_xGa_{4-x}$  alloys (BaAl<sub>4</sub> type) and for  $CeAu_{1.5}Ga_{2.5}$ (CaBe<sub>2</sub>Ge<sub>2</sub> type). The low temperature magnetization versus field data are shown in insets; open squares field up; full squares field down.



considered to be responsible for the non-linear variation of the unit cell dimensions with increasing Au content.

### 3.4. Magnetism

The magnetic behavior of the  $REAu_xGa_{4-x}$  alloys was investigated in the temperature range from 2 to 1100 K (see Figs. 3–5); paramagnetic parameters were obtained from a least-squares fit to a simple Curie–Weiss law and are listed in Table I.

*a. Alloys with  $BaAl_4$  type of structure.*  $LaAu_{0.6}Ga_{3.4}$  was found to be diamagnetic in the whole temperature range with a characteristic room temperature value of  $\chi_M = -2.42 \times 10^{-4} \text{ cm}^3/\text{mole}$ .

Magnetism of cerium-containing alloys  $CeAu_xGa_{4-x}$  ( $x = 0.35, 0.5, 0.6, 0.75, 1.0$ ) is essentially characterized by paramagnetic trivalent cerium. The susceptibilities closely follow a Curie–Weiss law, with small values of paramagnetic Curie temperatures  $\theta_p$  and effective paramagnetic mo-

ments ranging from  $2.44 \mu_B$  for  $x = 0.35$  to  $2.59 \mu_B$  for  $x = 1$ . The rise in  $\mu_{\text{eff}}$ , i.e., the percentage amount of  $Ce^{3+}$ , correlates with the observed increase in volume with increasing Au content. At low temperatures onset of ferromagnetic ordering is observed, with ordering temperatures linearly decreasing with increasing gold substitution. From isothermal magnetization curves versus magnetic field (see inset, Fig. 3) a saturation moment of  $1.22 \mu_B$  was determined in case of  $CeAu_{0.6}Ga_{3.4}$ , whereas the magnetic remanence appeared to be only ca. 50% of the magnetization in high field (3 T). Thus a very narrow hysteresis loop suggests the coercive field to be smaller than 0.1 T.

$PrAu_{0.75}Ga_{3.25}$  and  $NdAuGa_3$  alloys are paramagnetic above 80 K, with effective paramagnetic moments practically identical to ideal  $Pr^{3+}$ - and  $Nd^{3+}$ -free ion moments (see Table I and Fig. 4). The deflection of the inverse susceptibility data from the

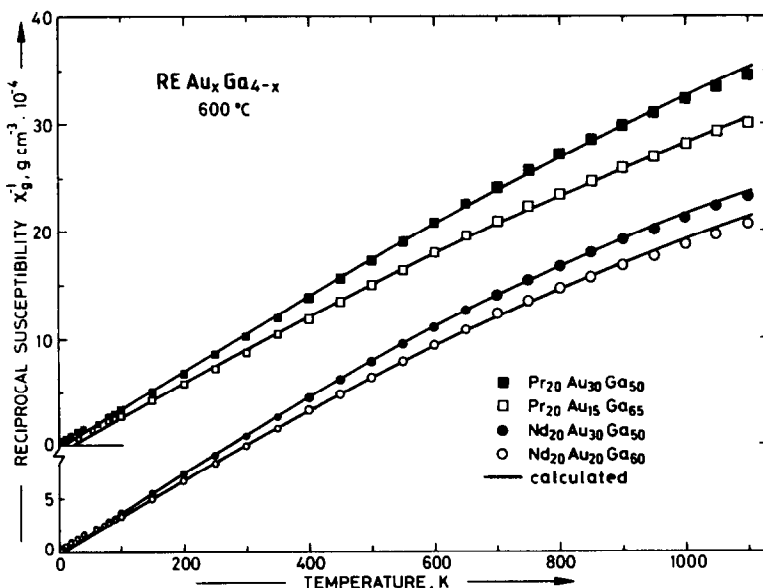


FIG. 4. Reciprocal gram-susceptibility versus temperature for  $(Pr,Nd)Au_xGa_{4-x}$  alloys ( $BaAl_4$  type,  $x = 0.75$  and  $x = 1.0$ , respectively) and  $(Pr,Nd)Au_{1.5}Ga_{2.5}$  ( $CaBe_2Ge_2$  type) and the calculated least-squares fit.

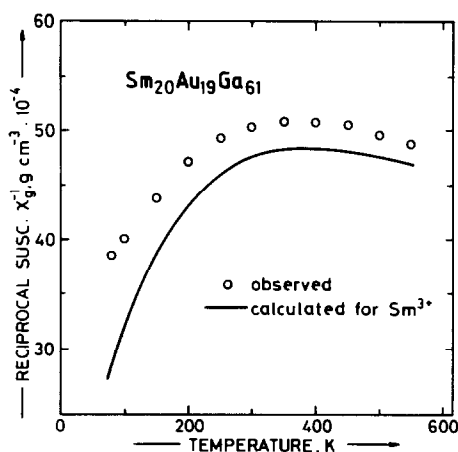


FIG. 5. Reciprocal gram-susceptibility versus temperature for  $SmAu_xGa_{4-x}$  ( $BaAl_4$  type); for comparison the calculated curve for ideal  $Sm^{3+}$  is shown by the solid line.

Curie-Weiss curve below 80 K probably indicates the onset of spontaneous magnetization at 7 and 4 K, respectively.

Since the ordering temperature of the  $(Ce, Pr, Nd)Au_xGa_{4-x}$  alloys approximately scale with the de Gennes factor  $(g_J - 1)^2 J(J + 1)$ , the indirect exchange interaction (5) is believed to induce the ferromagnetic transitions of the  $RE$  sublattices.

Magnetic susceptibilities for  $SmAu_{0.95}Ga_{3.05}$  reveal a Van Vleck-type paramagnetism of closely spaced multiplets as shown in Fig. 5.

*b. Alloys with  $CaBe_2Ge_2$  type of structure.* Magnetic properties of the  $RE Au_{1.5}Ga_{2.5}$  alloys with the  $CaBe_2Ge_2$  type of structure remain practically unchanged with respect to the  $BaAl_4$ -type compounds (see Figs. 3 and 4). No magnetic nor superconducting transition was observed down to 2 K. The paramagnetic parameters are listed in Table I.

### Acknowledgments

This research was supported by the Austrian Science Foundation (Fonds zur Förderung der wissenschaftlichen Forschung in Österreich) under Contract P5297. Thanks are due Dr. E. Gusset from Alcan Electronic Materials AG, Rohrschach, Switzerland, for the kind supply of the 4N-gallium. The single-crystal data collection was carried out on a STOE four-circle diffractometer of the Mineralogical Institute of the University of Vienna. We kindly thank Dr. E. Pertlik for technical assistance.

### References

1. YU. N. GRIN, K. HIEBL, AND P. ROGL, *J. Less-Common Met.* **110**, 299 (1985).
2. YU. N. GRIN, P. ROGL, K. HIEBL, AND R. EIBLER, *J. Less-Common Met.* **115**, 367 (1986).
3. YU. N. GRIN, K. HIEBL, P. ROGL, AND R. EIBLER, *J. Less-Common Met.* **118**, 335 (1986).
4. J. H. VAN VLECK, "The Theory of Electric and Magnetic Susceptibilities," Oxford Univ. Press (Clarendon), Oxford (1932).
5. H. PINTO, M. MELAMUD, M. KUZNIETZ, AND H. SHAKED, *Phys. Rev. B* **31**, 508 (1985).